THE JOURNAL OF PHYSICAL CHEMISTRY A LETTERS

2009, *113,* 8147–8151
Published on Web 07/01/2009

Degenerate Intermolecular and Intramolecular Proton-Transfer Reactions: Electronic Structure of the Transition States

Tarun K. Mandal

Department of Biotechnology, Haldia Institute of Technology, Hatiberia, Haldia 721657, West Bengal, India

Swapan K. Pati*

Theoretical Sciences Unit and DST Unit on Nanoscience, Jawaharlal Nehru Centre for Advanced Scientific Research. Jakkur Campus, Bangalore 560064, India

Ayan Datta*

School of Chemistry, Indian Institute of Science Education and Research Thiruvananthapuram, CET Campus, Thiruvananthapuram 695016, Kerala, India

Received: May 13, 2009; Revised Manuscript Received: June 15, 2009

Density functional theory (DFT) calculations are performed on a series of double and single proton-transfer reactions to study the variation in polarizations in complexes during the dynamics of proton transfer from one isoenergetic, hydrogen-bonded ground-state structure to the other. The isotropic average polarizability (α_{av}) shows an interesting single-humped profile with a maxima coinciding with the transition state of the reaction. Similar profiles are also computed at Nd:YaG frequencies. The origin of the maximal polarizability at the transition state is traced to maximal charge separation and large D (donor)−A (acceptor) distances. Maximal polarizability for the transition state suggests an interesting, novel, and less memory extensive computational tool to locate the transition state for hydrogen-transfer reactions in hydrogen-bonded complexes.

Proton-transfer processes are the most well-studied reaction mechanisms across various disciplines in chemistry, materials science, and biochemistry.[1−4] These processes have gained utmost importance since such reactions frequently occur in the cellular transport processes,[5,6] acid−base reactions,[7,8] redox processes,[9,10] and various excited-state processes including excited-state proton transfer (ESPT),[11,12] proton coupled electron transfer (PCET),[13−15] and vectorial proton transport across cell membranes.[16,17] The rate and dynamics of proton-transfer processes crucially depend on the detailed profile of the reaction barrier. Within the framework of the classical transition-state theory, the rate of the reaction is controlled by the barrier height.[18,19] Interestingly, a qualitative idea for the structure of the transition state (TS) can be derived from the well-known Hammond's postulate, which states that highly exothermic (endothermic) reactions have their TS similar in structure to that of the reactants (products).[20,21] In a similar spirit of the Hammond's postulate, one may postulate that for reactants and products that are equi-energetic and related through inversion of symmetry of the position of the proton, the TS should have the highest symmetry with translational equivalence from the reactant and product.

For a quantitative understanding of the structure of the transition state, knowledge about the location of the transition state is required, which can be obtained through calculation of the force constants for each bond and tracking the mode that softens and thereby gets an imaginary frequency.[22,23] However, for such calculations the computation effort increases by several orders of magnitude as the number of atoms in the molecule/cluster/assembly increases. In fact, the high computational demand for force-constant calculations renders direct "on-the-fly" calculation of the dynamics of proton-transfer reactions difficult even for moderately sized systems (>60 atoms) on the fastest of workstations. This has led to a bottleneck for ab initio computation of reaction dynamics of proton-transfer processes in many important biological molecules. In such a scenario, development of a computationally less-expensive tool to predict the structure of the transition state is essential. An additional requirement from such a new method would be that the method should have a direct correspondence with well-known chemically appealing qualitative tools like the Hammond postulate for a generalized understanding.

We have, in this manuscript, studied prototypical cases of intermolecular and intramolecular hydrogen-bonded dimers. The choice of the systems has been such that the reactant and products (related by inversion symmetry across the D−H···A bonds) are degenerate (D = A) so that only a single transition state connects them. For the intermolecular proton-transfer reactions, we have selected the formic acid dimer (FAD), the acetic acid dimer (AAD), and the trifluoroacetic acid dimer (F_3-AAD). On the other hand, 1,8-bis(diamino)naphthalene (proton sponge) is selected as an example of an intramolecular proton-transfer reaction. Our main result is that, for all the reactions that we have studied, we find that the transition state, (D−r_1---

* Corresponding authors. E-mail: A.D., ayan@iisertvm.ac.in; S.K.P., pati@jncasr.ac.in.

10.1021/jp9044513 CCC: $40.75

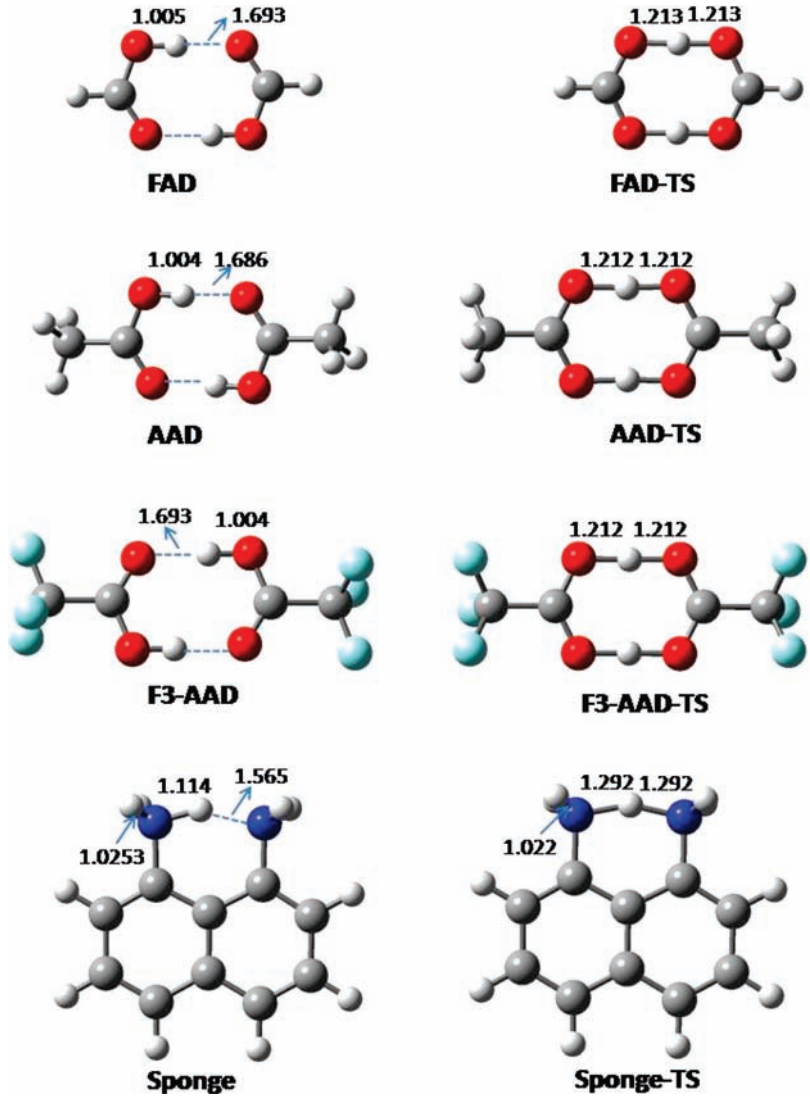

Figure 1. Optimized structures for formic acid dimer (FAD), acetic acid dimer (AAD), trifluoroacetic acid dimer (F3-AAD), sponge, and their respective transition states for proton transfer. The important D−H···A distances (in Å) are also reported.

H−r_2---A) with $r_1 = r_2$, has an average polarizability larger than that for a nonsymmetric position of the proton ($r_1 \neq r_2$) along the proton-transfer reaction coordinate. In the following sections, we discuss the computational methods, detailed results, and their analyses. Finally, we conclude the manuscript by a summary of our results and future prospects.

The geometries for all the ground-state structures of the hydrogen-bonded complexes have been optimized using the Becke 3 parameter Lee−Yang−Parr (B3LYP)[24] hybrid density functional theory (DFT) functional at the 6-31G(d) level of basis set.[25,26] Additional frequency calculations were performed on the minimum energy structures to confirm that these structures belong to the lowest energy minima. Translational symmetry was used to verify the equivalence of the reactants and the products in all aspects other than the position of the protons. The transition states are located by scanning the potential energy profile for various (D−r_1---H---A) by varying r_1. For all the structures, the TSs correspond to the symmetric hydrogen-bridged structures. The polarization responses are calculated at a frequency of 1064 nm, corresponding to the Nd:YaG laser using the formalism proposed by Snijders and Baerends.[27] All the frequency dependent polarizabilities are computed using the ADF package at the PW91/TZP level.[28] It is important to note that results for calculations of polarizabilities are quite dependent on the level of exchange and correlations.[29] Polarizability calculations at this level of theory have been recently shown to be quite accurate even for ionic molecules.[30] The average polarizibility, $\alpha_{av} = 1/3(\alpha_{xx} + \alpha_{yy} + \alpha_{zz})$ is calculated for each scan step to generate the profile for the variation in the polarizability with r_1. For the intermolecular double H-bonded complexes, the scans are performed by simultaneous, equivalent and opposite increases in r_1 for both the H-bonds.

In Figure 1, the structures for the ground-state H-bonded complexes and their TS for the degenerate transfer of hydrogen are shown. There are several interesting features in the structural aspects for the ground-state and the transition-state geometries between intramolecular and intermolecular cases. For all the three intermolecular H-bonded complexes and their transition states, the D−H···A and the D···H···A distances are similar. However, the structure for the intramolecular case (sponge) and its TS show quite different hydrogen-bonded profiles. A scan for the rotation of the NH_3^+ group along the plane of the naphthalene ring leads to a barrier height of 7.53 kcal/mol, which is in marked contrast to the almost barrierless rotation (~0.14 kcal/mol) for the methyl group in toluene.[31−33] Thus, the presence of the hydrogen bond, N−H···N, substantially stabilizes the system. In harmony with the strong H-bond in the proton sponge, the ground state has its N−H bond involved in

the N−H···N hydrogen bonding, thereby elongating substantially (by ∼0.09 Å, red-shifted) in comparison to the other two "free" N−H bonds. The origin for the stronger hydrogen bonds can be understood on the basis of the small N···N distance of 2.679 Å for the H-bonded complex. Interestingly, the O···O distances are 0.11 Å more for the O−H···O bonds in FAD, AAD, and F_3-AAD. This is counterintuitive as the O−H···O bonds are known to be stronger than N−H···N bonds and O···O distances are mostly smaller than N···N distances.[34,35] The reason for the opposite behavior in the proton sponge is rationalized on the basis of the fact the N···N atoms are actually confined in space by their additional connectivity with the 1,8-ends of naphthalene molecules. Such, quantum confinement mediated shortening of D···A distances with concomitant increase in H-bond energy has been known earlier.[36,37]

For FAD, AAD, and F_3-AAD, our B3LYP/6-31G(d) calculations predict dimerization energy (ΔE) and barrier height ($\Delta E^{\ddagger}$) as −15.26 and +7.70 kcal/mol; −15.53 and +7.71 kcal/mol; −14.93 and +7.67 kcal/mol, respectively. The dimerization energies are corrected for basis-set superposition error (BSSE) using the counterpoise-correction method.[38] The dimerization energies for the three complexes follow the order of electronegativity of the substituents. The +I effect of a $-CH_3$ group stabilizes the H-bonded complex while the −I effect of a $-CF_3$ destabilizes it (by reducing the electron density on the D/A ends) in comparison to FAD. Thus, the stability of the complexes follows the order AAD > FAD > F_3-AAD. For FAD, previous calculations at the MP2/6-31G(d,p) level predict ΔE and $\Delta E^{\ddagger}$ = −16.4 and +8.0 kcal/mol, respectively.[39,40] For AAD, previous calculations at the RI MP2/augTZVPP level predict $\Delta E = -14.74$.[41] Thus, our calculated dimerization energies and the barrier heights for the intermolecular reactions are in good agreement with previously known results.

On the other hand, the barrier height for the intramolecular proton-transfer reaction is found to be very low. At the B3LYP/6-31G(d) level, we find $\Delta E^{\ddagger}$ for the sponge case to be 0.79 kcal/mol, which further reduces to 0.69 kcal/mol at the B3LYP/6-31+G(d,p) level. Thus, degenerate proton transfer is readily accessible at room temperature. The origin of such a low barrier height can be understood on the basis of the fact that the N−H bond length increases by only 0.178 Å for going from the ground state to the transition state without any significant geometry changes in other portions of the molecule. However, for the intermolecular hydrogen-transfer molecules, the O−H bond stretches by +0.208 Å from the ground state to the transition state. Also, interestingly, the $-CH_3$ and $-CF_3$ groups undergo a conformational change from staggered to eclipsed in the process of climbing to the barrier-top in cases of AAD and F_3-AAD, respectively. Thus, the effective geometry reorganization for GS → TS is minimal for sponge.

Nevertheless, the elongation of the D−H bond in D−H···A to D···H in D···H···A for all the molecules suggests that there should be an increase in charge separation as well. This is in agreement with the maximum polarity of the transition state as observed in the Mulliken charges. Thus, one expects that the bond moment of the D−H bond would increase as one stretches the D−H bond to go to the TS. However, the transition states being centrosymmetric, the overall dipole moment reduces to zero in TS for all the molecules. Also, for the intermolecular double-H-bonded molecules, inversion symmetry ensures zero dipole moments for the ground state as well. Thus, intuitively, one expects two distinctly different behaviors for the profile of the dipole moment in the intramolecular and intermolecular H-bonded molecules for GS → TS. While observation of such single-minima and triple-minima profiles in dipole moment (for D−H···A to D···H···A to D−H···A) for intramolecular and intermolecular H-bonded molecules respectively is an interesting experimental challenge (through IR spectroscopy), it lacks the simplicity of generalization. One expects a similar behavior in the first hyperpolarizability (β) as well since the symmetry arguments are similar.[42]

However, a more elegant approach for studying the variation in the properties of H-bonded complexes as they go from GS to TS irrespective of whether they are intermolecular or intramolecular can be derived by investigating the average polarizability (α_{av}) along the reaction path. Polarizability, being an even-order derivative of energy with respect to the applied electric field, has a nonzero value for even centrosymmetric molecules. Also, from an experimental viewpoint, anisotropic polarizability (because of the planarity of the molecules that leads to zero polarizations in the $\perp^r$ axis along the plane of the molecule) ensures that all the states from GS → TS can be traced by Raman spectroscopy. Polarizability has also been shown to minimize for maximally stable species/isomers and lowest energy transition states.[43]

In Figure 2, the profile for the variation in the average polarizability, α_{av} (in au), with respect to the increase in the D−H distance for all four systems considered in this study are shown. At each step of the scan, α_{av} is calculated for zero field, $\alpha_{av}(0)$, and at Nd: YaG frequency, $\alpha_{av}(\omega)$, λ = 1064 nm (1.67 eV), a wavelength suitable for many HRS experiments.[44] For both zero frequency and Nd: YaG frequency, the average polarizability increases as the GS structure climbs the barrier to reach the TS. At a given D−H distance, $\alpha_{av}(\omega) > \alpha_{av}(0)$, since at a larger field strength more excited states will be accessible, leading to more charge separation. α_{av} reaches a maximum value at the TS followed after which it decreases in the same manner (not shown) following the inversion symmetry of the molecule. An analysis of the individual tensor elements shows that $\alpha_{in\text{-}plane} = 1/2(\alpha_{xx} + \alpha_{yy})$ is the major component for the average polarizability. While all the intermolecular H-bonded complexes show similar profiles, the case for the intramolecular aggregate is both qualitatively and quantitatively different. Unlike the intermolecular aggregates, the sponge shows an almost linear increasing relationship with increasing D−H bond length without reaching a plateau near the TS. The slope for the increase in α_{av} is much smaller in the sponge for an initial increase in the D−H bond length from the GS. This is readily understood since, in the sponge, there is only one D−H···A bond while, in the intermolecular H-bonded complexes, two D−H···A bonds are polarized simultaneously with increasing the D−H bond lengths. Thus, the effective $\Delta\alpha_{av}$ are less in the sponge for equivalent distortions.

It would also be interesting to study the variation in α_{av} for nonsymmetric proton-transfer reactions where the location of the transition state becomes qualitatively different due to the absence of translational symmetry. We have considered the reaction dynamics of the mixed H-bonded complex, formic acid···acetic acid. ΔE (BSSE corrected) and $\Delta E^{\ddagger}$ for this complex are found to be −15.49 and +7.55 kcal/mol, respectively, at the same level of theory as described earlier. In Figure 3, the profile for the variation in the average polarizability, α_{av} (in au), with respect to the increase in the O−H distance of acetic acid is shown. For both zero-field and Nd: YaG frequencies, the maximum value for polarizability along the reaction coordinate corresponds to the transition-state structure, as also found for the symmetric proton-transfer cases.

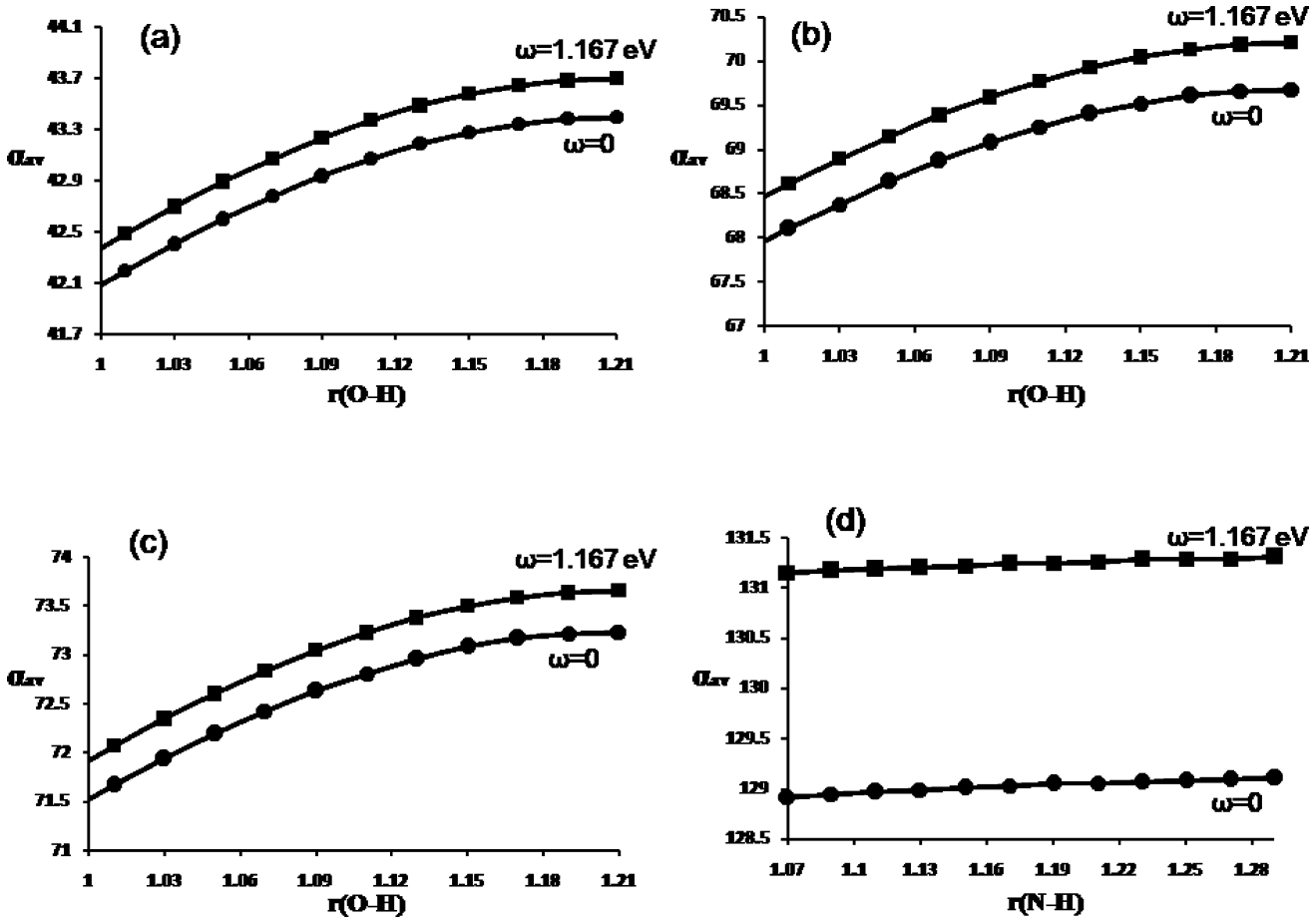

Figure 2. Profiles for variations in average polarizability, α_{av} (in au), for (a) formic acid dimer (FAD), (b) acetic acid dimer (AAD), (c) trifluoroacetic acid dimer (F3-AAD), and (d) sponge, with increasing D−H distances (in Å) for D−H···A.

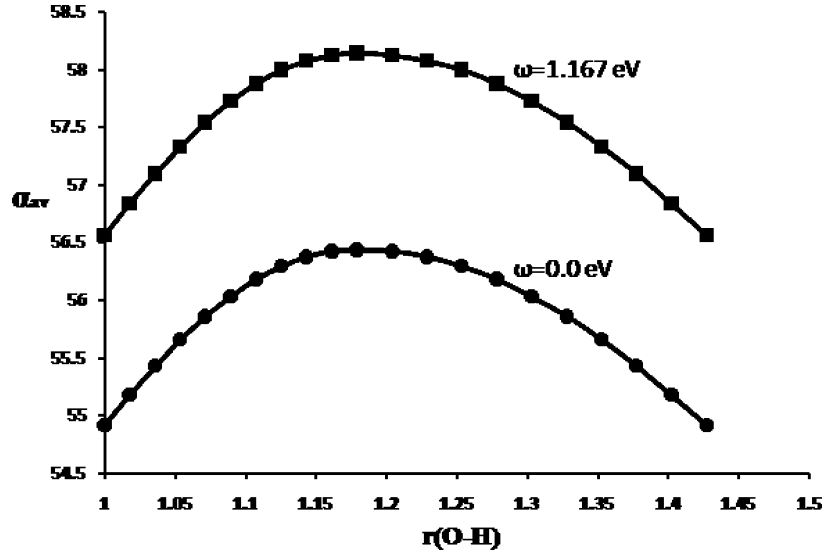

Figure 3. Profiles for variations in average polarizability, α_{av} (in au), for the formic acid···acetic acid complex with increasing O−H distances of acetic acid (in Å).

From the present computational study it is clear that in the reaction coordinate for degenerate proton transfer, the transition state has the highest average polarizability irrespective of the nature of the H-bonded complexes (intramolecular or intermolecular). There are important consequences of our finding. The postulate that maximum polarizability is reached at the transition state can be utilized to qualitatively locate the transition state without undertaking a detailed calculation of the force constants unless specifically required. The computational advantage for such an endeavor is substantial.[45] More significantly, in our opinion, the postulate of maximum polarizability at the transition state provides a conceptually lucid description of the transition state. The concept is based on the general chemical intuition that transition states have at least one bonding parameter (like a bond, angle, or dihedral angle) that is substantially different from that of the ground-state structure. Such geometries are

expected to have larger charge separation and thus greater polarizations. We believe that our arguments for locating the transition states are qualitatively complementary to the well-accepted Hammond's postulate in organic chemistry and be further developed into a robust computational tool to locate the transition state.

Supporting Information Available: Ground-state optimized geometries, frequencies, and complete ref 26. This material is available free of charge via the Internet at http://pubs.acs.org.

Acknowledgment. T.K.M. thanks Haldia Institute of Technology for the research leave. S.K.P. thanks DST, CSIR, for funding. A.D. thanks DST Fast-track scheme for partial funding.

References and Notes

(1) Schowen, R. L.; Klinman, J. P.; Hynes, J. T. *Hydrogen-Transfer Reactions*; Wiley-VCH: New York, 2006.

(2) Scheiner, S. *Hydrogen Bonding: A Theoretical Perspective*; Oxford University Press: Oxford, U.K., 1997.

(3) Desiraju, G.; Steiner, T. *The Weak Hydrogen Bond: Applications to Structural Chemistry and Biology*; Oxford University Press: Oxford, U.K., 1999.

(4) Jeffrey, G. A. *An Introduction to Hydrogen Bonding*; Oxford University Press: Oxford, U.K., 1997.

(5) (a) Deisenhofer, J.; Michel, H. *EMBO J.* **1989**, *8*, 2149. (b) Pederson, B. P.; Buch-Pederson, M. J.; Morth, J. P.; Palmgren, M. G.; Nissen, P. *Nature* **2007**, *450*, 1111.

(6) (a) Gust, D.; Moore, T. A.; Moore, A. L. *Acc. Chem. Res.* **2001**, *34*, 40. (b) Hamp, N. *Chem. Rev.* **2000**, *100*, 1755.

(7) (a) Orth, E. S.; Brandao, T. A. S.; Milagre, H. M. S.; Eberlin, M. N.; Nome, F. *J. Am. Chem. Soc.* **1943**, *65*, 803. (b) Guo, H.; Wlodawer, A.; Guo, H. *J. Am. Chem. Soc.* **2005**, *127*, 15662.

(8) (a) Alverez, A. V.; Sordo, J. A.; Scuseria, G. E. *J. Am. Chem. Soc.* **2005**, *127*, 11318. (b) Adhikary, A.; Kumar, A.; Khundari, D.; Sevilla, M. D. *J. Am. Chem. Soc.* **2008**, *130*, 10282. (c) Mallajosyula, S. S.; Pati, S. K. *J. Phys. Chem. B* **2007**, *111*, 11614.

(9) (a) Soper, J. D.; Kryatov, S. V.; Rybak-Alkimova, E. V.; Nocera, D. G. *J. Am. Chem. Soc.* **2007**, *129*, 5069. (b) Rhile, I. J.; Mayer, J. M. *J. Am. Chem. Soc.* **2004**, *126*, 12718.

(10) (a) Zhu, X.-Q.; Zhang, M.-T.; Yu, A.; Wang, C.-H.; Cheng, J.-P. *J. Am. Chem. Soc.* **2008**, *130*, 2501. (b) Murata, T.; Morita, Y.; Yumi, Y.; Fukui, K.; Yamochi, H.; Saito, G.; Nakasuji, K. *J. Am. Chem. Soc.* **2007**, *129*, 10837.

(11) (a) Frutos, L. M.; Markmann, A.; Sobolewski, A. L.; Domcke, W. *J. Phys. Chem. B* **2007**, *111*, 6110. (b) Schmidtke, S. J.; Underwood, D. F.; Blank, D. A. *J. Am. Chem. Soc.* **2004**, *126*, 8620.

(12) (a) Ludlow, M. K.; Skone, J. H.; Hammes-Schiffer, S. *J. Phys. Chem. B* **2008**, *112*, 336. (b) Ghosh, A. K.; Schuster, G. B. *J. Am. Chem. Soc.* **2006**, *128*, 4172.

(13) (a) Mayer, J. M.; Hrovat, D. A.; Thomas, J. L.; Borden, W. T. *J. Am. Chem. Soc.* **2002**, *124*, 11142. (b) Mader, E. A.; Davidson, E. R.; Mayer, J. M. *J. Am. Chem. Soc.* **2007**, *129*, 5153. (c) Wu, A.; Mayer, J. M. *J. Am. Chem. Soc.* **2008**, *130*, 14745.

(14) (a) Hammes-Schiffer, S. *Acc. Chem. Res.* **2001**, *34*, 273. (b) Ishikita, H.; Soudackov, A. V.; Hammes-Schiffer, S. *J. Am. Chem. Soc.* **2007**, *129*, 11146. (c) Carra, C.; Iordanova, N.; Hammes-Schiffer, S. *J. Am. Chem. Soc.* **2003**, *125*, 10429.

(15) (a) DiLabio, G. A.; Ingold, K. U. *J. Am. Chem. Soc.* **2005**, *127*, 6693. (b) DiLabio, G. A.; Johnson, E. R. *J. Am. Chem. Soc.* **2007**, *129*, 6619. (c) Lingwood, M.; Hammond, J. R.; Hrovat, D. A.; Mayer, J. M.; Borden, W. T. *J. Chem. Theory Comput.* **2006**, *2*, 740.

(16) (a) El-Sayed, M. A. *Acc. Chem. Res.* **1992**, *25*, 279. (b) Stoeckenius, W. *Acc. Chem. Res.* **2008**, *130*, 2436.

(17) (a) Uhl, R.; Abrahamson, E. W. *Chem. Rev.* **1981**, *81*, 291. (b) Gascon, J. A.; Sproviero, E. M.; Batista, V. S. *Acc. Chem. Res.* **2006**, *39*, 184. (c) Rando, R. R. *Chem. Rev.* **2001**, *101*, 1881.

(18) Laidler, K. J. *Theories of Chemical Reaction Rates*; McGraw-Hill: New York, 1969.

(19) Lagana, A.; Lendvay, G. *Theory of Chemical Reaction Dynamics*; Springer: Berlin, 2004.

(20) (a) Hammond, G. S. *J. Am. Chem. Soc.* **1955**, *77*, 334. (b) Yarnell, A. *Chem. Eng. News* **2003**, *81*, 42.

(21) Solomons, T. W. G.; Fryhle, C. B. *Organic Chemistry*, 8th ed.; Wiley: New York, 2003.

(22) Lewars, E. *Computational Chemistry: Introduction to the Theory and Applications of Molecular and Quantum Mechanics*; Springer: Berlin, 2003.

(23) Cramer, C. J. *Essentials of Computational Chemistry: Theories and Models*, 2nd ed.; Wiley: New York, 2004.

(24) (a) Becke, A. D. *J. Chem. Phys.* **1993**, *98*, 5648. (b) Lee, C.; Yang, W.; Parr, R. G. *Phys. Rev. B* **1988**, *37*, 78.

(25) Hariharan, P. C.; Pople, J. A. *Theor. Chem. Acta.* **1973**, *28*, 213.

(26) Frisch, M. J.; et al. *Gaussian 03*; Gaussian, Inc.: Wallingford, CT, 2003.

(27) (a) van Gisbergen, S. J. A.; Snijders, J. G.; Baerends, E. J. *Phys. Rev. Lett.* **1997**, *78*, 3097. (b) van Gisbergen, S. J. A.; Snijders, J. G.; Baerends, E. J. *J. Chem. Phys.* **1998**, *109*, 10644.

(28) (a) Velde, G. t.; Bickelhaupt, F. M.; van Gisbergen, S. J. A.; Guerra, C. F.; Baerends, E. J.; Snijders, J. G.; Ziegler, T. *J. Comput. Chem.* **2001**, *22*, 931. (b) ADF2008.01, SCM; Theoretical Chemistry, Vrije Universiteit: Amsterdam, The Netherlands, http://www.scm.com.

(29) (a) Maroulis, G.; Karamanis, P.; Pouchan, C. *J. Chem. Phys.* **2007**, *126*, 154316. (b) Maroulis, G. *J. Chem. Phys.* **2008**, *129*, 044314. (c) Karamanis, P.; Pouchan, C.; Maroulis, G. *Phys. Rev. A* **2008**, *77*, 013201.

(30) Datta, A. *J. Phys. Chem. B* **2009**, *113*, 3339.

(31) Lambrt, J. B.; Nienhuis, R. J.; Finzel, R. B. *J. Phys. Chem.* **1981**, *85*, 1170.

(32) Pitzer, K. S.; Scott, D. W. *J. Am. Chem. Soc.* **1943**, *65*, 803.

(33) Eliel, E. L.; Wilen, S. H. *Stereochemistry of Organic Compounds*; John Wiley and Sons: New York, 1994.

(34) (a) Kollman, P. A.; Allen, L. C. *Chem. Rev.* **1972**, *72*, 283. (b) Etter, M. C. *Acc. Chem. Res.* **1990**, *23*, 120.

(35) (a) Desiraju, G. R. *Acc. Chem. Res.* **1996**, *29*, 441. (b) Steiner, T. *Angew. Chem., Int. Ed.* **2002**, *41*, 48.

(36) (a) Shemeema, O.; Ramachandran, C. N.; Sathymurthy, N. *J. Phys. Chem. A* **2006**, *110*, 2. (b) Ramachandran, C. N.; Sathyamurthy, N. *Chem. Phys. Lett.* **2005**, *410*, 348.

(37) (a) Mohan, P. J.; Datta, A.; Mallajosyula, S. S.; Pati, S. K. *J. Phys. Chem. B* **2006**, *110*, 18661. (b) Datta, A.; Pati, S. K. *Int. Jour. Quant. Chem.* **2006**, *106*, 1697.

(38) (a) *Molecular Electronic - Structure Theory*; Helgaker, T., Jorgensen, P., Olsen, J., Eds.; John Wiley & Sons: New York, 2000. (b) Boys, S. F.; Bernardi, F. *Mol. Phys.* **1970**, *19*, 553.

(39) Tautermann, C. S.; Loferer, M. J.; Voegele, A. F.; Liedl, K. R. *J. Chem. Phys.* **2004**, *120*, 11650.

(40) Kim, Y. *J. Am. Chem. Soc.* **1996**, *118*, 1522.

(41) Chocholousova, J.; Vacek, J.; Hobza, P. *J. Phys. Chem. A* **2003**, *107*, 3086.

(42) (a) Datta, A.; Pati, S. K. *J. Phys. Chem. A* **2004**, *108*, 9527. (b) Pati, S. K.; Ramasesha, S.; Shuai, Z.; Bredas, J. L. *Phys. Rev. B* **1999**, *59*, 14827. (c) Datta, A.; Pati, S. K. *Chem. Soc. Rev.* **2006**, *35*, 1305 and references therein.

(43) (a) Hohm, U. *J. Phys. Chem. A* **2000**, *104*, 8418. (b) Le, T. N.; Nguyen, L. T.; Chandra, A. K.; De Proft, F.; Geerlings, P.; Nguyen, M. T. *J. Chem. Soc., Perkin Trans.* **1999**, *2*, 1249.

(44) Das, P. K. *J. Phys. Chem. B* **2006**, *110*, 7621 and references therein.

(45) A simple test job for a H_2O molecule was performed in a single Intel core-2-duo processor with 2.4 GHz clock speed and 1 GB RAM. For the same external memory provided, a polarizability calculation in G03 at B3LYP/6-31G(d) level takes a CPU time of 3.0 s while a frequency calculation at the same level of theory takes 7.0 s.

JP9044513